

## IMPACT OF ELECTROMAGNETIC LOSSES IN CLOSED TWO-COMPONENT MAGNETIC SHIELDS ON THE AMPACITY OF UNDERGROUND POWER CABLES

Juan Carlos del Pino-López<sup>1, \*</sup>, Pedro Cruz-Romero<sup>1</sup>, and Luis Serrano-Iribarnegaray<sup>2</sup>

<sup>1</sup>Department of Electrical Engineering, University of Seville, Camino de los Descubrimientos s/n, Seville 41092, Spain

<sup>2</sup>Department of Electrical Engineering, Polytechnic University of Valencia, Camino de Vera, s/n, Valencia 46022, Spain

**Abstract**—In this paper two typical arrangements of underground single-core high voltage three-phase power cables (flat and trefoil protected by PVC pipes) inside a closed shield of three different materials (low-carbon steel, non-oriented grain steel and aluminium) are analysed. The shield has two components: a U-shaped base and a flat plate (cover) located on top of the base. Whereas most of previous papers on this subject only dealt with the degree of mitigation obtained with each material, this paper, in addition to also addressing this issue, mainly focusses on the effect that electromagnetic losses induced in the shield have on the ampacity of the cable and the cost involved (material and losses). To obtain the numerical results, a high number of simulations by a well-known commercial finite element method software (COMSOL Multiphysics) have been performed. The results obtained in the numerous cases analysed are widely commented and the solutions that enable an important mitigation with no current derating and at a comparatively low cost are highlighted.

### 1. INTRODUCTION

In the last decades several proposals have been published to mitigate the magnetic field (MF) generated by underground cables, undesirable in certain circumstances (proximity of dwellings, disruptive effects in sensitive equipment, etc.). In particular, one design that has raised a certain interest in the scientific community is the shield composed

---

*Received 23 November 2012, Accepted 26 December 2012, Scheduled 2 January 2013*

\* Corresponding author: Juan Carlos del Pino-Lopez (vaisat@us.es).

by two parts: a U-shape base and a flat plate (cover) located on top of the base, obtaining a closed shield. This design, proposed in [1] for ferromagnetic materials, has the advantage over previous closed shields of simplifying the laying procedure and the subsequent maintenance operations, keeping meanwhile the typical high MF mitigation of closed shields compared with open ones. Moreover, it does not require welding because each of the longitudinal sections of the shield (of about 1 m) has a conical shape so that it can be partially overlapped to the next one.

This solution has been installed in several real lines in the last years. In [2] three applications in Italy are described (trefoil configuration at 132 and 380 kV), obtaining a shielding effectiveness SE (ratio between the non-mitigated field and the mitigated one in dB) greater than 25 dB. On the other hand, in [3] several experiments of installation of a similar ferromagnetic shield in a 150 kV line in Belgium are described, comprising both trefoil and flat configurations and different thicknesses. The SE obtained was around 26 dB. In this work the use of aluminium was also tested, obtaining a lower SE = 18 dB.

Regarding the losses generated by this kind of shield, in [4] an in-depth analysis is performed, comparing the losses dissipated by three types of material: two ferromagnetic materials of different magnetic permeabilities and aluminium. The main conclusion is that if losses must be limited aluminium is the best choice, provided that its lower mitigation compared with high-permeability material is enough.

The importance of minimizing electromagnetic losses is associated to two important issues that must be taken into account. On one side, these losses can cause an additional temperature rise in the conductors, leading to a current reduction of the line. On the other side, these losses increase the operational cost of the line over all the years of operation. Therefore it is crucial to know how to reduce the induced losses into the screen in order to reduce both issues.

To this end, in this paper we go a step further by performing an in-depth parametric analysis by means of 2-D finite element method (FEM) models, developed to show the influence of the geometrical parameters of the shield not only on the MF mitigation achieved, but also on the electromagnetic losses induced in the shield and their influence on the carrying capacity of the mitigated line. Furthermore, the economic cost of the shield is studied, taking into account both the material cost and the losses cost over all the years of operation. In this sense, three types of material are considered: a low-carbon steel, a non-oriented grain steel and aluminium. In order to analyse the worst situation (from the thermal point of view), either a flat or trefoil

configuration of the power cables will be considered installed into PVC pipes.

## 2. FEM MODEL

The problem to be solved is rather complex, since there are two physics involved: an electromagnetic problem coupled to a thermal one. In addition, the complex geometrical shape of the screen requires the use of numerical techniques. In this situation the best choice is to use a FEM formulation for a suitable modelling of the system to be studied in order to compute either the mitigated MF [5–7] or the temperature of the power cables [7–9]. The mathematical models to be solved are described in the following sections.

### 2.1. Electromagnetic Problem

The mitigated MF is computed by means of a FEM model based on the following assumptions:

- 1) The cables are straight and infinitely long, thereby rendering the problem 2-D.
- 2) All materials have constant electrical properties, with the exception of conductive materials (conductors and screen), whose electrical conductivity  $\sigma(\theta)$  depends on temperature:

$$\sigma(\theta) = \frac{\sigma_0}{1 + \alpha(\theta - 20)} \quad (1)$$

where  $\theta$  is the unknown temperature and  $\sigma_0$  and  $\alpha$  are the conductivity and the temperature coefficient of the material at 20°C, respectively.

- 3) The electrical conductivity of mother soil is ignored.
- 4) The phase currents are sinusoidal and balanced.

In this situation, the equation to be solved can be described as

$$\nabla \times \left( \frac{1}{\mu} \nabla \times \vec{A} \right) + j\omega\sigma\vec{A} = \vec{J}_e \quad (2)$$

where  $\vec{A}$  is the magnetic vector potential,  $\omega$  the angular frequency,  $\sigma$  the conductivity,  $\mu$  the permeability, and  $\vec{J}_e$  the external current density. To take into account the nonlinear behaviour of ferromagnetic materials,  $\mu$  will be considered as a function of the flux density.

For better understanding, the shielding effectiveness of the shield is quantified in terms of the ratio between the resulting (root sum square) nonmitigated and mitigated MFs in dB:

$$SE(x, y) = 20 \cdot \log \left( \frac{\left| \vec{B}_p(x, y) \right|}{\left| \vec{B}_s(x, y) \right|} \right) \quad (3)$$

where  $\vec{B}_p$  is the MF generated by the power cables and  $\vec{B}_s$  the mitigated field.

The power losses generated in the cables and in the shield will be used as the heat input for the thermal problem. In particular, eddy current losses ( $P_e$ ) can be calculated from the total current density  $\vec{J}$  as follows:

$$P_e = \int \frac{\vec{J} \cdot \vec{J}^*}{\sigma} dS \quad (4)$$

On the other hand, the losses generated in nonlinear ferromagnetic materials are also considered. These losses can be conceptually separated into three loss components, known as the hysteresis  $P_h$ , classical eddy current  $P_e$ , and additional losses  $P_a$  [10]. Considering Steinmetz's [11–13] and Bertotti's [13, 14] equations, the total losses can be described as

$$P = P_h + P_e + P_a = K_h f^a B_m^b + P_e + K_a f^{1.5} B_m^{1.5} \quad (5)$$

where  $P_e$  can be computed by (4),  $B_m$  is the maximum flux density,  $K_h$  is the hysteresis loss coefficient,  $K_a$  is the additional loss coefficient, and  $a$  and  $b$  are constants. The latter coefficients are obtained from information provided by the manufacturer.

## 2.2. Thermal Problem

The starting assumptions for the thermal problem are as follows:

- 1) Since power cables are straight and infinitely long, the heat transfer problem can be formulated in 2D on the  $x$ - $y$  plane.
- 2) The temperature gradient in the soil at great distance (25 m) from the cables is zero.
- 3) Power cables are buried in homogeneous soil.
- 4) All materials have constant thermal properties, including the thermal resistivity of the soil, since no moisture migration is considered.
- 5) The effect of radiation at the ground surface is neglected.
- 6) The soil temperature at a depth of 15 m is known ( $\theta_s$ ).

- 7) The heat flux at soil surface is transferred by convection, with known convection heat transfer coefficient ( $h$ ) and temperature of the air ( $\theta_a$ ) [15].
- 8) Heat radiation is present between the outer cable surface and the inner pipe surface, with known surface emissivity ( $\varepsilon$ ) of the materials [15].
- 9) The air region inside the plastic pipes is a closed system, so heat convection is present. The mass conservation, momentum conservation and energy conservation equations must be solved [8].

As a consequence, the associated steady-state heat conduction equation can be expressed [15] as

$$\frac{\partial}{\partial x} \left( \frac{1}{\rho} \frac{\partial \theta}{\partial x} \right) + \frac{\partial}{\partial y} \left( \frac{1}{\rho} \frac{\partial \theta}{\partial y} \right) + q = 0 \tag{6}$$

where  $q$  is the heat source generated by the power cables and the shield (computed from the electromagnetic problem),  $\theta$  is the unknown temperature, and  $\rho$  is the thermal resistivity of each material.

The coupled electromagnetic-thermal problem is iteratively solved as there are temperature-sensitive elements, such as the electrical conductivity of the conductors and the shield, which must be continuously corrected for the newly calculated temperature.

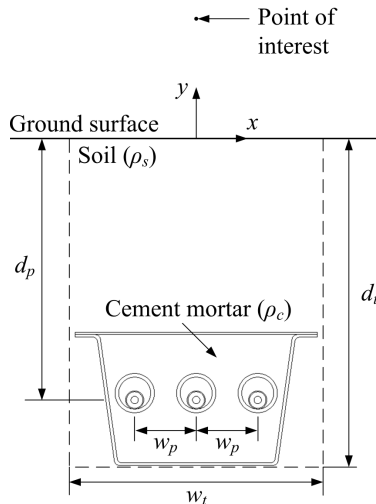


**Figure 1.** Underground phase conductors, screen and trench dimensions.

**Table 1.** Parameters of the power cable (copper) and pipes.

Conductor diameter (mm)	30.2	DC Resistance of conductor (20°C) ( $\Omega/\text{km}$ )	0.0274
XLPE insulation thickness (mm)	18.25	Insulation thermal resistivity ( $\text{K}\cdot\text{m}/\text{W}$ )	3.5
Copper sheath thickness (mm)	0.45	Copper sheath Section ( $\text{mm}^2$ )	95
PVC jacket thickness (mm)	3.2	Jacket thermal resistivity ( $\text{K}\cdot\text{m}/\text{W}$ )	6
Cable external diameter (mm)	74	Copper thermal resistivity ( $\text{K}\cdot\text{m}/\text{W}$ )	0.0025
Copper thermal coefficient $\alpha$ ( $^{\circ}\text{C}^{-1}$ )		0.00393	
Pipe external diameter (mm)	160	PVC thermal resistivity ( $\text{K}\cdot\text{m}/\text{W}$ )	6
Pipe internal diameter (mm)	140	PVC emissivity	0.9

### 3. CASE STUDY 1: POWER CABLES IN FLAT CONFIGURATION

Two situations are discussed in this research. The first one concerns about a closed shield installed to mitigate the MF generated by a 132 kV underground three-phase power system placed in flat configuration, as shown in Fig. 1. Phase conductors are installed in PVC pipes having an external diameter of 160 mm, with a separation of  $w_p = 25$  cm, buried at a depth of  $d_p = 1.25$  m and have a cross-section of  $630 \text{ mm}^2$ , with the electrical and thermal parameters shown in Table 1. Trench dimensions are  $w_t = 1.1$  m and  $d_t = 1.6$  m.

On the other hand, the values of the thermal resistivity of the soil is  $\rho_s = 1.25 \text{ K}\cdot\text{m}/\text{W}$ , and the temperature of the soil at a depth of 15 m is  $\theta_s = 10^{\circ}\text{C}$ . The convection heat transfer coefficient at soil surface

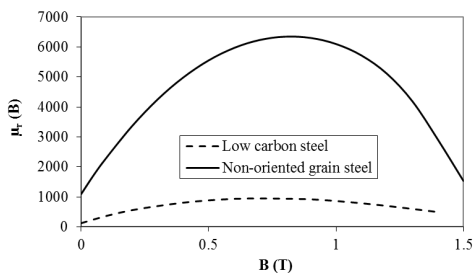


**Figure 2.** Relative permeability of the employed steels.

is  $h = 25 \text{ W/m}^2 \cdot \text{K}$  and the air temperature  $\theta_a = 25^\circ\text{C}$ . Finally, the surface emissivity of the outer cable surface and the inner duct surface (both are PVC) is  $\varepsilon = 0.9$ . In this situation, the ampacity of the line is about 809 A when there is no shield installed, in accordance with the IEC 60287 standard, since the permissible operating temperature is  $\theta_m = 90^\circ\text{C}$  (cable insulation is XLPE). Therefore this value will be considered as the current flowing through the line in the parametric analysis.

The shield is initially considered to have the following dimensions taken as a reference: a 3 mm thickness, a base width of about 660 mm, a height of 532 mm and the cover of 1040 mm. Once the power cables are installed into the shield, it is filled with cement mortar, which has a thermal resistivity of  $\rho_c = 0.83 \text{ K}\cdot\text{m/W}$ .

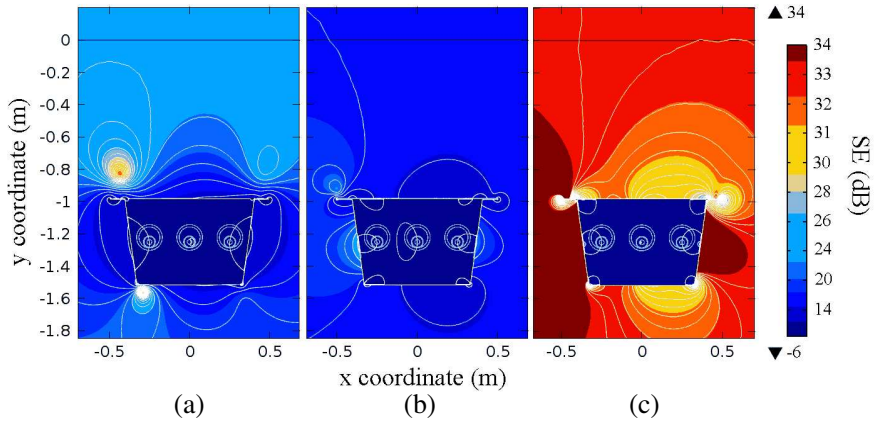
Three materials are employed in the shield: aluminium (Al), a low-carbon steel (LCS) and a non-oriented grain steel (NOS). Their electrical and thermal parameters are shown in Table 2, which includes the coefficients needed to compute the hysteresis and additional losses by Equation (5) (data obtained from the manufacturer). Since both steels are nonlinear ferromagnetic materials, its relative permeability is a function of the flux density  $\mu_r(B)$ , as shown in Fig. 2.

These materials have been selected since they can provide SE values higher than 0 dB in any point of the external area out of the shield (hence the MF has been reduced), as shows Fig. 3, where it is represented the SE field provided by the shield with each material. Also, Fig. 3 shows a remarkable efficiency obtained with NOS shield compared to aluminium and LCS shields.

Regarding the relative position between the shield and the phase conductors, in the parametric analysis it will be assume that the shield is approximately centered with the power cables (the bottom of the shield is about 0.2 m away from the cables center), as shown in Fig. 1, although it is easier to lay them directly on the bottom of the shield.

**Table 2.** Parameters for the various materials used in the shield (20°C).

Material	Density (kg/m <sup>3</sup> )	$\sigma$ (S/m)	$\mu_r$	$\rho$ (K·m/W)	$\alpha$ (°C <sup>-1</sup> )
Aluminium	2700	$38 \cdot 10^6$	1	0.00625	0.004
Low carbon steel	7580	$6.5 \cdot 10^6$	$\mu_r (B)$	0.0125	0.005
Non-oriented grain steel	7700	$2.3 \cdot 10^6$	$\mu_r (B)$	0.03	0.005
Material	$K_h$	$a$	$b$	$K_a$	
Aluminium	–	–	–	–	
Low carbon steel	0.045	1.15	1.35	0.0045	
Non-oriented grain steel	0.0109	1.234	1.775	$4.4 \cdot 10^{-4}$	

**Figure 3.** SE field and iso-lines for shields made of (a) aluminium, (b) low carbon steel and (c) non-oriented grain steel.

This is because in this situation the maximum temperature of the cables is the lowest possible without having a negative influence on the SE achieved with the three materials used, as shown in Fig. 4, where it is represented the evolution of the SE achieved at the point of interest situated at 1 m above ground surface (Fig. 1) and the maximum temperature of the cables when the separation from the bottom of the shield is increased.

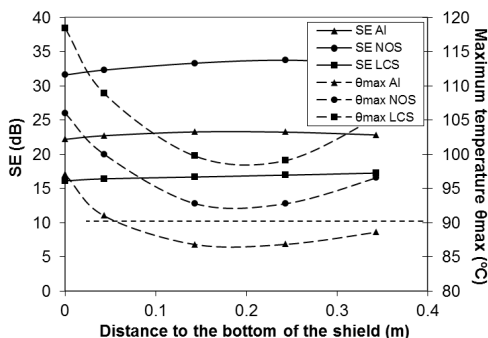


**Figure 4.** Evolution of the SE (at 1 m above ground surface) and the maximum temperature of the cables with their separation from the bottom of the shield (3-mm thickness).

**Table 3.** Evolution of the electromagnetic losses induced in the shield (3-mm thickness) with the distance between cables and the bottom of the shield for the three materials used.

Distance (m)	Aluminium	Low carbon steel			Non-oriented grain steel		
	$P_e$ (W/m)	$P_h$ (W/m)	$P_a$ (W/m)	$P_e$ (W/m)	$P_h$ (W/m)	$P_a$ (W/m)	$P_e$ (W/m)
0	36.52	18.15	6.20	52.25	16.61	4.32	49.91
0.05	19.91	14.83	4.92	37.87	9.06	1.16	22.86
0.1	11.05	10.72	3.34	24.15	7.19	0.96	14.64
0.2	9.21	10.31	3.17	22.62	7.14	0.96	13.99
0.3	12.41	13.27	4.25	30.42	12.72	1.47	24.39

As can be seen, the SE remains constant, or even increases, when power cables are separated from the bottom of the shield, while their temperature decreases. In particular, when aluminium is used, the temperature of the cables can even decrease below the maximum temperature of 90°C. This way the effect on the ampacity of the line is minimum. This is partially caused by the lower electromagnetic losses that are induced in the shield when the conductors are farther from its bottom, as shown in Table 3, where each term of the induced losses decreases with higher distances and are minimum at about 0.2 m of separation. In this sense, it should be remarked that the induced losses on steel shields are more important than those on the aluminium shield for the same shield size, as will be seen again through the parametric analysis. In addition, when the shield is centered with the line, the

temperature also decreases because there is more amount of cement mortar surrounding the power cables, whose lower thermal resistivity helps to better cool the power cables.

### 3.1. Parametric Analysis

The following parametric analysis involves both geometrical and economical parameters, focusing on those aspects which directly influence the cable ampacity and the total cost associated with a particular size of the shield. In this sense, only one dimension is revised on each analysis, leaving the other dimensions at the reference values. When necessary, the shield size is modified by several scaling factors applied either to the height or the width or to both dimensions (referenced as height scaling factor, width scaling factor and total scaling factor, respectively). It must be noticed that is crucial to evaluate separately the effects of each of the geometrical parameters in order to establish the dimensions of the shield which achieve the best shielding effectiveness without limiting the ampacity of the line. This is described in the following sections for the example shown in Fig. 1.

#### 3.1.1. Influence of Shield Thickness

For the shield dimensions mentioned earlier, Fig. 5 shows the evolution of the SE in the point of interest (at 1 m above ground surface and in the vertical of the central conductor) and the maximum temperature of the cables with the thickness of the shield. As can be observed, better mitigation results are obtained when using NOS shields, followed by aluminium and LCS, both of them providing similar mitigation levels

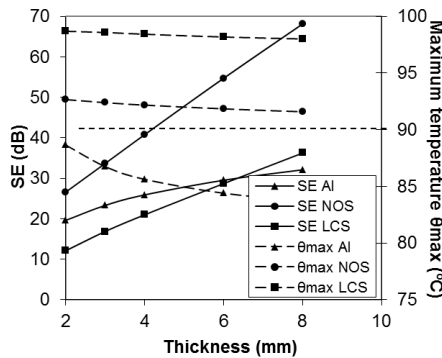


**Figure 5.** Evolution of the SE (at 1 m above ground surface) and the maximum temperature of the cables with the thickness of the shield.

**Table 4.** Total power losses induced in the shield (W/m) for various thicknesses.

Thickness (mm)	Al	LCS	NOS
2	14.39	34.69	21.36
3	10.56	35.33	21.41
4	8.33	35.66	21.49
6	5.92	36.12	21.68
8	4.69	36.48	21.87

depending on the shield thickness. However, in this particular case only the aluminium shield will not have a negative impact on the ampacity of the line, since the maximum temperature of the cables remains always below  $90^{\circ}\text{C}$  when this material is used. Furthermore, this effect is more important when the thickness increases, which not only improves the mitigation level, but can also cool power cables below its initial temperature when there is no shield installed (e.g., a 4-mm aluminium shield leads to a temperature of the phase conductors of  $86^{\circ}\text{C}$ , lower than the initial value of  $90^{\circ}\text{C}$  for a current of 809 A). This behavior is not only explained by the lower power losses induced in the aluminium shield when increasing its thickness (Table 4), but also because there is much more amount of good thermally conductor material (aluminium) that helps to evacuate the heat from the cables. So if necessary, using a suitable thickness on an aluminium shield would avoid overheating of the cables.

On the other side, although a greater thickness of the shield also leads to better SE values when using NOS or LCS, the maximum temperature on the conductors remains almost constant and higher than  $90^{\circ}\text{C}$  in both materials. This is because the induced electromagnetic losses in both materials are quite higher than those of the aluminium shield, as shown in Table 4. However, despite these higher losses, the maximum temperature of the conductors slightly decreases thanks to the thermal properties of both steels and cement mortar. So, the ampacity of the line should be reduced in order to avoid overheating of the cables, especially in the case of LCS as the maximum temperature should be decreased in about  $8^{\circ}\text{C}$ .

Taking all this into account, it can be concluded that the only way to limit the impact on the cable's ampacity when using NOS or LCS shields may be by modifying the size of the shield, since greater thicknesses seem to have no significant effects. This is developed next.

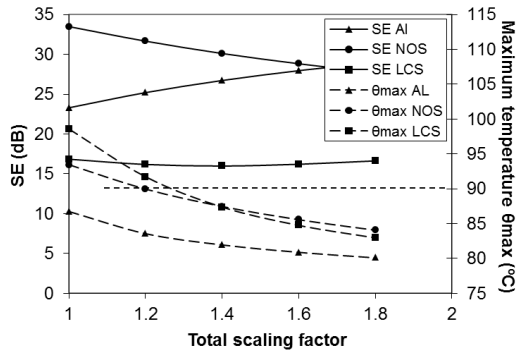


**Figure 6.** Evolution of the SE (at 1 m above ground surface) and the maximum temperature of the cables with the size (total scaling factor) of the shield.

### 3.1.2. Influence of Shield Size

The size of the shield can be modified by applying a scaling factor simultaneously to both the height and the width of the shield, but without changing its thickness. Fig. 6 shows how the SE and the maximum temperature of the conductor vary when increasing the shield size (increasing the total scaling factor for a shield thickness of 3 mm). It is easily observed how in general NOS shields provide a higher mitigation efficiency than aluminium and LCS due to its higher relative permeability. But Fig. 6 also shows that bigger shields made of any of the three materials leads to lower temperatures, and hence this helps us to limit the impact on the ampacity of the line. Again, this reduction on the temperature is caused by two effects: the lower induced losses in the shield and the presence of a higher amount of materials which have good thermal properties (shield and cement mortar).

However, the SE evolves in different ways on each material. So, while the SE remains almost constant in the case of LCS, in the case of NOS shields it decreases strongly. On the contrary, the mitigation efficiency of aluminium shields are much better with higher thicknesses.

Nevertheless, it should be clarified that the size of the shield is limited by trench dimensions and, hence, this parameter cannot be set as freely as desired. So it may be of importance to study the influence of the shape of the shield in order to adjust the shield into the limits of the trench, for example by modifying separately the height or the width of the shield, as developed next.

3.1.3. Influence of the Width and the Height of the Shield

If a scaling factor is only applied to the height of the shield, the evolution of the SE and the maximum temperature of the cables is shown in Fig. 7(a) (for a shield thickness of 3 mm), where a scaling factor below 1 means that the shield height has been reduced from the reference value defined earlier (532 mm). As can be seen, the lower the height, the higher the maximum temperature is, especially in the cases of steel shields. This is due to the higher electromagnetic losses that are induced in the shield when its top and bottom plates get closer to the phase conductors (Table 5). However, this effect is less important in the aluminium shield, as induced losses increase more slowly with this parameter (Table 5). So if needed, only in this case it would be possible to reduce the height of the shield with a limited impact on the current-carrying capacity of the line, but the SE would also be reduced.

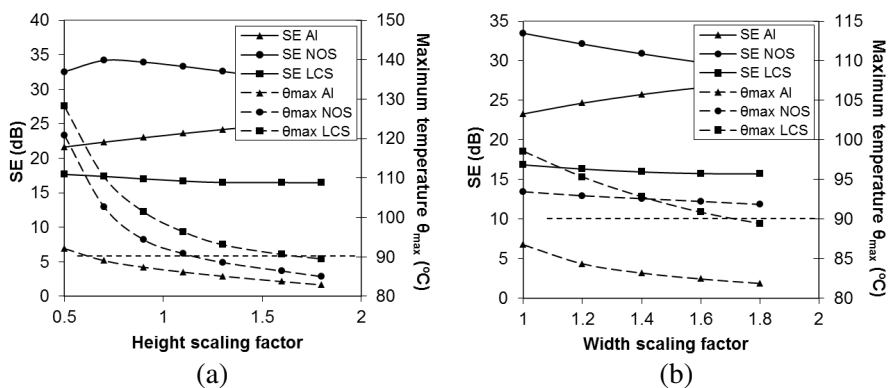


Figure 7. Evolution of the SE (at 1 m above ground surface) and the maximum temperature of the cables with (a) the height and (b) the width of the shield.

Table 5. Total power losses in the shield (W/m) for various shield heights.

Height scaling factor	Aluminium	Low carbon steel	Non-oriented grain steel
0.5	18.74	88.53	70.77
0.9	11.41	40.46	25.48
1.3	8.76	26.11	15.14
1.5	7.91	22.89	12.86

In any case, increasing the height of the shield tends to diminish the influence of the shield losses on the ampacity of the mitigated line when using any of the three materials, while their mitigation levels remain quite constant (case of NOS and LCS shields) or even increase (aluminium shield). However, as it has been observed along this study, LCS shields have always the lowest SE values and the higher impact on the temperature of the phase conductors.

In relation to the shield width (Fig. 7(b)), results are very similar to those of the previous section, where the maximum temperature can be reduced if the shield width is incremented, mainly with the LCS and aluminium shields. However, this effect is less important in the case of NOS shields, since the maximum temperature remains almost constant when modifying this parameter.

Therefore, from this parametric analysis it can be concluded that a suitable shape and size of the shield can provide enough mitigation levels with a minimum effect, or even no effect, on the current rating of the power cables. An optimization study is required to take into account all the geometrical parameters involved.

### 3.2. Shield Cost

When selecting the shield to be installed in a particular place, not only the mitigation levels and the impact on the line ampacity must be taken into account, but also its cost, which includes the cost of the material and losses cost over the years of operation. The final goal is to find the aluminium or steel shield with the best balance between shielding effectiveness and cost.

So, from the parametric analysis developed previously, it can be derived that using a shield size of 1.3 times greater than the dimensions taken as a reference it is possible to keep the ampacity of the line in the initial 809 A, since phase conductors will have a temperature lower than 90°C (Fig. 6). In this way, it is possible to compare the shield cost for each material without worrying about the line temperature. To do that, it is considered a line length of 100 m to be shielded, obtaining the total cost of the shield (material and losses) over a period of 30 years as stated in the IEC 60287 for the cost of power cables [16]. Reference data are: 2600 euro/t for aluminium; 600 euro/t for LCS; 900 euro/t for NOS; energy price: 0.1 euro/ton; discount rate: 5%; energy cost rate: 2%; and demand charge: 0.03 euro/W·year.

In this situation, Fig. 8(a) shows the evolution of the SE and the total cost of the shield for different thicknesses of each material. It is easily observed that the total cost associated to the aluminium shield is the cheapest choice, although aluminium is the most expensive material from those considered. On the contrary, the cheapest materials (both

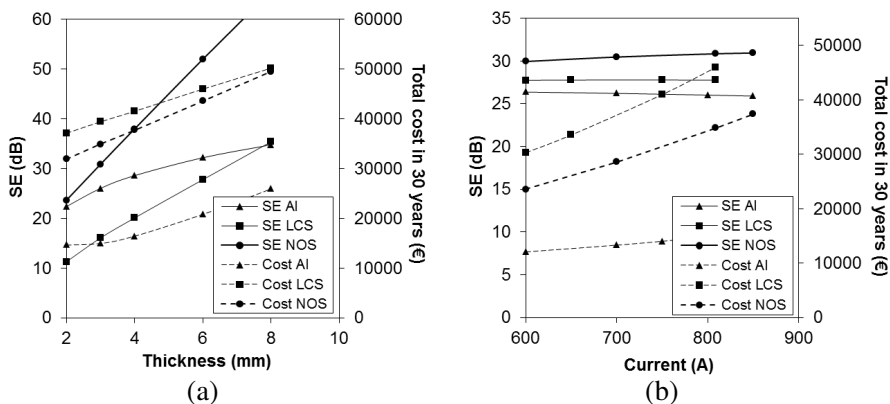


**Figure 8.** Evolution of the SE (at 1 m above ground surface) and the total cost of 100 m of shield (total scaling factor of 1.3) with (a) the thickness of the shield and (b) the current through the line.

**Table 6.** Total cost of different shields (euro) over 30 years as a function of the minimum mitigation requirements.

SE <sub>min</sub> (dB)	Aluminium	Low carbon steel	Non-oriented grain steel
26	15,356	46,456	32,756
28	17,102	48,342	34,127
29.5	18,672	48,832	36,032
31	19,705	49,462	36,851

steels) leads to a total cost about two times more expensive than the aluminium shield. This is due to the higher electromagnetic losses induced on the steel shields, which greatly increase the final cost.

Taking all this into account, if a minimum mitigation level of 26 dB is required in a particular place, different options can be deduced from Fig. 8(a), selecting the suitable thickness for each material to meet the mitigation requirements. In this case, it would be needed a 3 mm thick aluminium shield, a 6 mm thick LCS shield and a 2.5 mm NOS shield. The cost associated to these shields are listed in Table 6, where it is also shown the total cost of the shields when meeting higher mitigation requirements.

This way, although NOS shield is the better choice in terms of shielding effectiveness, the aluminium shield seems to be the optimum choice since it provides enough mitigation levels to comply the mitigation requirements with the lowest cost possible.

Figure 8(a) is computed considering that the current flowing through the line is equal to its ampacity (809 A), which is the most critical situation. But this current may vary being usually lower and hence modifying both the mitigation efficiency and the total cost associated with the shield. This is shown in Fig. 8(b) for the shield solutions that comply with a minimum SE of 26 dB (Table 6), where it is represented the evolution of SE and the total cost of the shield with the line current. As can be seen, when the line current is lower than 809 A the SE values of aluminium and LCS shields increase slightly, while it is worsened in NOS shields. In any case, the mitigation levels remain high. In addition, the total cost for the three materials diminishes with the current, since the induced electromagnetic losses do so.

### 3.3. Comparison with Open Shields

From the previous section it can be concluded that an aluminium shield may be the best choice due to its balance between shielding effectiveness and cost. However, it may be of interest to compare this solution with others that are usually employed in underground power cables in flat configuration. In particular, an aluminium open shield in H-layout can provide important mitigation levels close to those of the closed shield [7]. This is shown in Fig. 9, where it is represented the evolution of the SE and the total cost of both shields for a range of thicknesses that have no effect on the ampacity of the line. It is easily observed that both solutions can provide similar results in terms of

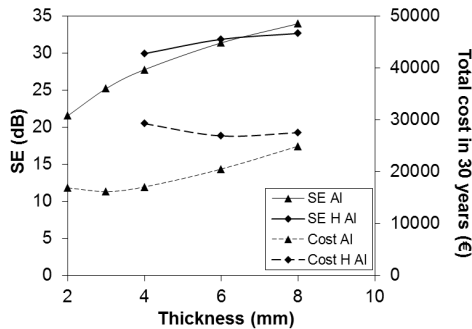


**Figure 9.** Evolution of the SE (at 1 m above ground surface) and the total cost of 100 m of shield with the thickness of the plates used in an aluminium closed shield (total scaling factor of 1.3) and a H-layout open shield (vertical plates of 1-m length separated by 1 m; horizontal plate of 0.9 m length and situated at 0.12 m above cables).

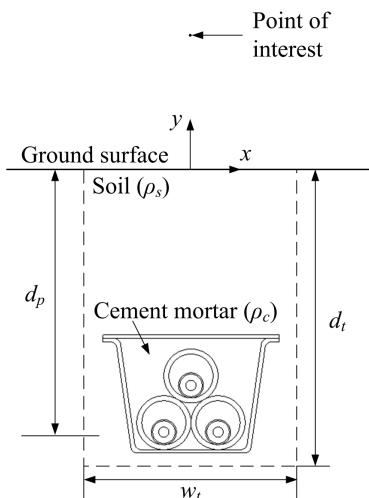


**Figure 10.** Underground power cables in trefoil configuration inside the shield.

mitigation levels, but the closed shield is still cheaper than the H-layout, although the difference is not as remarkable as that observed in Fig. 8(a) when using NOS or LCS closed shields. So, the H-layout still is a solution of interest to be taken into account, specially when trench dimensions are restricted, since its width is only about 1 m, lower than that of the closed shield that is about 1.35 m.

#### 4. CASE STUDY 2: POWER CABLES IN TREFOIL CONFIGURATION

The second study included in this research is in relation with the same type of shield applied to the same 132 kV power line, but in this case the line is laid in trefoil configuration, as shown in Fig. 10.

Again, phase conductors are installed into 160 mm PVC pipes, which are in contact. All the boundary conditions for the electromagnetic and thermal problems are identical to those used in the study case 1, but this leads to a new ampacity value for the line in trefoil configuration, which is about 765 A, value that is considered to be flowing through the line in the parametric analysis. For the rest, all dimensions and parameters of the system remain the same, except for the shield size taken as a reference, which in this case is initially considered to have a 3 mm thickness, a base width of 350 mm, a height of 340 mm and the cover is 560 mm wide. This way, the shield

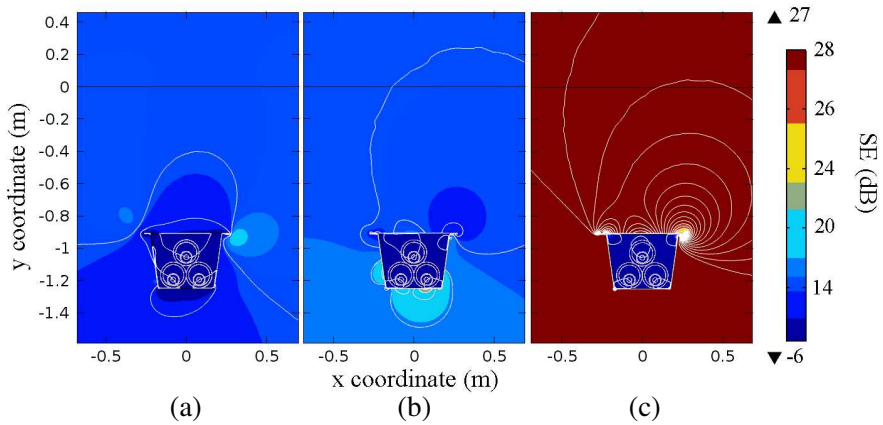


**Figure 11.** SE field and iso-lines for shields made of (a) aluminium, (b) low carbon steel and (c) non-oriented grain steel.

is adjusted to the line size in order to simplify the laying process to ensure the trefoil configuration, as described in [1, 2].

A new parametric analysis is developed next using also aluminium (Al), a low carbon steel (LCS) and a non-oriented grain steel (NOS), with the electrical and thermal parameters shown in Table 2 and Fig. 2. Again, these materials have been selected since they can provide relevant mitigations levels ( $SE > 0$  dB) nearby the point of interest situated at 1 m above ground surface, especially in the case of NOS shield, as shown in Fig. 11.

Regarding the relative position between the shield and the power cables, contrary to that observed in the case study 1, there are no significant differences in the SE and the temperature of the cables whether the shield is centered or not with them, since there are lower losses induced in the shield due to the compact configuration of the line (Fig. 10). So, in our analysis we will assume the conductors installed at the bottom of the shield due to the easiness to lay them.

## 4.1. Parametric Analysis

### 4.1.1. Influence of Shield Thickness and Size

If only the shield thickness is varied, the SE and the maximum temperature on the phase conductors evolve as shown in Fig. 12(a). In this case, the worst mitigation results are presented for the aluminium shield, which barely reaches mitigations levels of 21 dB when using a thickness of 8 mm. In the same way, the LCS shield has poor mitigation

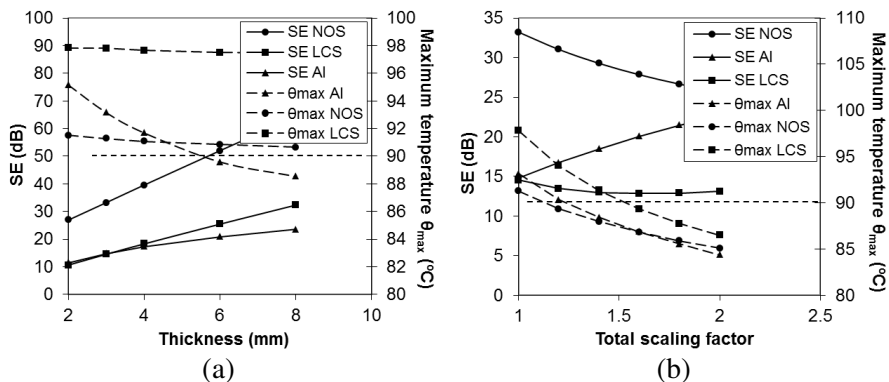


**Figure 12.** Evolution of the SE (at 1 m above ground surface) and the maximum temperature of the cables with (a) the thickness and (b) the size of the shield.

levels if low thicknesses are used, but its SE improves when using values higher than 5 mm. On the contrary, the NOS shield is always able to reach values of SE far above 26 dB. Nevertheless, only when using aluminium it is possible not to overheat the power cables employing a greater thickness. So NOS shields, and particularly LCS shields, have to be carefully considered as they may cause an important current rating reduction of the power line.

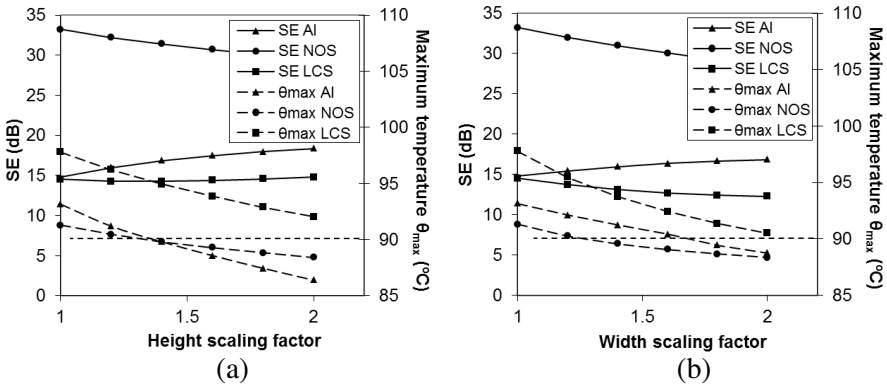
Therefore, it may be of interest to visualize the effects on the SE and the maximum temperature when a bigger shield is installed. This is shown in Fig. 12(b), where the thickness of the shield is fixed to 3 mm. It is clear that only the aluminium shield improves its SE with the shield size, while it worsens on both steels, especially on the NOS shield. Regarding the impact on the maximum temperature of the cables, it can be easily limited by slightly increasing the shield size when using aluminium or NOS, although it is also possible in LCS shields employing a much bigger shield. This is caused by the higher electromagnetic losses generated in the LCS shield, as shown in Table 7.

#### 4.1.2. Influence of Shield Width and Height

The influence of both the shield height and width are shown in Figs. 13(a) and 13(b) respectively, for a thickness of 3 mm. It is easily observed that both dimensions have similar effects on the SE provided by each material, where only the mitigation efficiency of the aluminium shield slightly improves while it remains constant for the LCS case and strongly decreases for the NOS shield.

**Table 7.** Total power losses induced in the shield (W/m) for various shield sizes.

Total scaling factor	Aluminium	Low carbon steel	Non-oriented grain steel
1	16.22	22.91	8.34
1.3	14.81	18.35	7.31
1.6	14.42	16.27	6.72
2	14.11	14.35	6.19

**Figure 13.** Evolution of the SE (at 1 m above ground surface) and the maximum temperature of the cables with (a) the height and (b) the width of the shield.

So the only important advantage obtained from increasing one of these dimensions is that it helps us to limit the impact on the ampacity of the line, as can be seen in Figs. 13(a) and 13(b). However, each material has a different reaction to these actions. For example, it seems that aluminium shields reach lower temperatures faster when increasing the shield height instead of increasing its width. On the contrary, the temperature seems to diminish faster when increasing the width on LCS or NOS shields. This behaviour is related not only with the electromagnetic losses induced on each material (Table 8), but also with their thermal properties.

## 4.2. Shield Cost

The economic analysis developed for this case study has been performed with the same data listed in the corresponding section of the

**Table 8.** Total power losses in the shield (W/m) for various shield widths.

Width scaling factor	Aluminium	Low carbon steel	Non-oriented grain steel
1	16.22	22.91	8.34
1.3	16.35	19.83	7.86
1.6	16.60	18.17	7.79
2	16.72	16.78	7.61

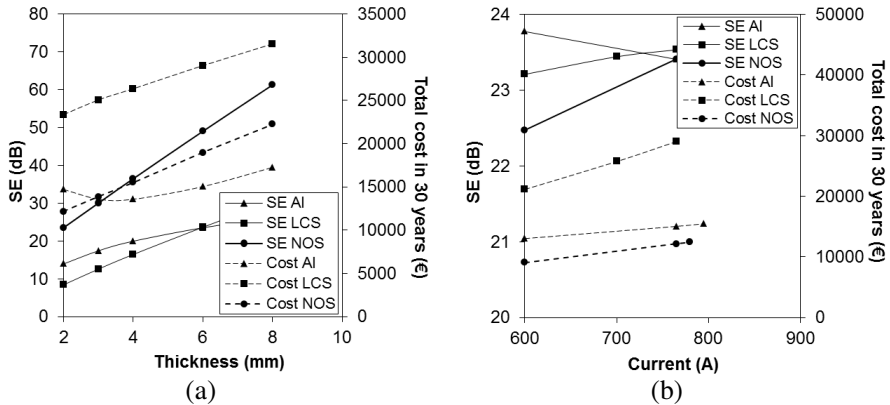


**Figure 14.** Evolution of the SE (at 1 m above ground surface) and the total cost of 100 m of shield (total scaling factor of 1.3) with (a) the thickness of the shield and (b) the current through the line.

case study 1 (material and energy cost). However it is again necessary to select a particular size for the shield in order to avoid the current derating of the power line. In this sense, a shield size of 1.3 times the size taken as a reference is selected. This shield is supposed to be installed along a line length of 100 m.

With these data, Fig. 14(a) shows the most important results when the shield thickness is increased. In particular the evolution of the SE and the total cost of the shield over 30 years of operation. It can be seen that the higher cost is obtained when using LCS to make the shield, which is about 1.6 times higher than the cost associated to the cheapest option (aluminium). Moreover, the shielding efficiency of both materials are very similar, so it is clear that LCS shields would be rejected. However, the cost of NOS shield is quite close to that of aluminium shield, especially at lower thickness, and they provide much higher efficiency levels than the aluminium.

**Table 9.** Total cost of different shields (euro) over 30 years as a function of the minimum mitigation requirements.

$SE_{\min}$ (dB)	Aluminium	Low carbon steel	Non-oriented grain steel
26	17,262	29,365	13,164
28	21,125	29,867	13,465
29.5	23,864	30,035	13,839
31	25,746	31,854	14,265

Considering all this, if a minimum SE of 26 dB is required, it would be necessary to choose the suitable thickness for each material to meet this constraint. In our case this leads to a NOS shield of 2.5 mm, a LCS shield of 7 mm and an aluminium shield of 9 mm. The total cost associated to these configurations is listed in Table 9, which also includes the total cost for other requirements of SE.

As can be concluded, for any  $SE_{\min}$  the best choice in this case is to use a NOS shield, since it complies with the mitigation requirements with the lowest cost possible. In any case, the total costs shown in Fig. 14(a) have been computed for a current flowing through the cables equal to its ampacity (765 A), which is the most critical situation. In fact, the current is usually lower. So this is considered in Fig. 14(b), where it is shown the influence of the current of the line in the mitigation efficiency and the cost of the shield when a  $SE_{\min} = 26$  dB is required. It is easily observed that, in general, the current through the cables has no important effects on both parameters, except for the case of LCS shields, whose SE can be lower than 26 dB if the current flowing through the line is about 700 A or less. But also, for this material the total cost of the shield decreases faster than the cost of the other materials when the current is lower.

## 5. CONCLUSIONS

The shielding effectiveness of a closed two-component magnetic shield and the impact of the induced electromagnetic losses on the total shield cost and the ampacity of the power cables have been studied for two cases of an underground power line, installed in flat and trefoil configuration, both protected by PVC pipes. Three different materials for the shield have been considered in the study (aluminium, a low carbon steel and non oriented grain steel), which is performed by means of a FEM electromagnetic-thermal coupled model.

A parametric analysis has been developed for the selected configurations of the line, concluding that the geometrical parameters of the shield have significant effects not only on the shielding effectiveness, but also on the ampacity of the shielded line and the shield cost (including material and losses cost over the years of operation). Tables and curves with comparative data presented in this paper help to select the suitable dimensions of a shield to be placed in a particular situation, in order to obtain the best mitigation levels and the lowest impact on the current rating of the mitigated line. In this sense, it has to be noticed that, in general, a greater size of the shield leads to a lower impact on the current rating of the mitigated line, but this also leads to a lower mitigation efficiency when using steel.

From all the materials considered to make the shield, this study concludes that aluminium provides significant mitigation levels with the lowest cost possible when shielding a line in flat configuration. Its mitigation efficiency is even close to that observed in other high efficiency open shields frequently used in lines laid in flat configuration, like the H-layout, but with a lower cost. However, if higher values of mitigation are needed, a non-oriented grain steel shield may be selected to be installed next to the line, but in this case the total cost of the shield is about twice of the aluminium.

On the other hand, if the line is laid in trefoil formation, a shield made of non-oriented grain steel is the best choice, since it provides very high mitigation levels with a reasonable cost, which is similar to the total cost of aluminium shields. However, in this situation aluminium shields cannot provide such high mitigation levels as those of the non-oriented grain steel.

Finally, in all the studied cases it is noticed that low carbon steel shields can provide significant mitigation levels when using a high value of thickness, but its cost is quite high compared to those of the other materials considered, which makes this material not to be best choice in any of the studied configurations.

## ACKNOWLEDGMENT

This work has been supported by the Spanish Ministry of Science & Innovation under grant ENE2010-18867 and by the regional Government of Andalucía under grant P09-TEP-5170.

## REFERENCES

1. Maioli, P., E. Borghi, F. Donazzi, and S. Belli, "Method for shielding the magnetic field generated by an electrical

- power transmission line and electrical power transmission line so shielded,” Patent, International Publication Number: WO 2005/013450 A1, Feb. 2005.
2. Conti, R., F. Donazzi, P. Maioli, R. Rendina, and E. A. Sena, “Some Italian experiences in the utilization of HV underground cable systems to solve local problems due to magnetic field and other environmental issues,” *Cigré Session*, Paper C4-303, 2006.
  3. De Wulf, M., P. Wouters, P. Sergeant, L. Dupré, E. Hoferlin, S. Jacobs, and P. Harlet, “Electromagnetic shielding of high-voltage cables,” *J. Magn. Magn. Mater.*, Vol. 316, 908–911, 2007.
  4. Sergeant, P. and S. Koroglu, “Electromagnetic losses in magnetic shields for buried high voltage cables,” *Progress In Electromagnetics Research*, Vol. 115, 441–460, 2011.
  5. Xu, X. and X. Yang, “A hybrid formulation based on uniform unimoment method or investigating the electromagnetic shielding of sources within a steel pipe,” *Progress In Electromagnetics Research*, Vol. 12, 133–157, 1996.
  6. Xu, X.-B. and G. Liu, “A two-step numerical solution of magnetic field produced by ELF sources within a steel pipe,” *Progress In Electromagnetics Research*, Vol. 28, 17–28, 2000.
  7. Del Pino, J.-C. and P. Cruz, “Influence of different types of magnetic shields on the thermal behaviour and ampacity of underground power cables,” *IEEE Trans. on Power Delivery*, Vol. 26, No. 4, 2659–2667, 2011.
  8. Liang, Y., “Steady-state thermal analysis of power cable systems in ducts using streamline-upwind/Petrov-Galerkin finite element method,” *IEEE Trans. on Dielectrics and Electrical Insulation*, Vol. 19, No. 1, 283–290, 2012.
  9. Anders, G.-J., M. Chaaban, and N. Bedard, “New approach to ampacity evaluation of cables in ducts using finite element technique,” *IEEE Trans. on Power Delivery*, Vol. 2, 969–975, 1987.
  10. Bertotti, G., *Hysteresis in Magnetism*, Academic Press, San Diego, 1998.
  11. Ionel, D.-M., M. Popescu, S. J. Dellinger, T. J. E. Miller, R. J. Heideman, and M. I. McGilp, “On the variation with flux and frequency of the core loss coefficients in electrical machines,” *IEEE Trans. on Industry Applications*, Vol. 42, No. 3, 658–667, 2006.
  12. Lee, P.-K., K. C. Kuo, C. J. Wu, Z. T. Wong, and J. Y. Yen, “Prediction of iron losses using the modified Steinmetz equation

- under sinusoidal waveform,” *Proceedings of 2011 8th Asian Control Conference (ASCC)*, 579–584, 2011.
13. Öztürk, N. and E. Çelik, “Application of genetic algorithms to core loss coefficient extraction,” *Progress In Electromagnetic Research M*, Vol. 19, 133–146, 2011.
  14. Bertotti, G., “General properties of power losses in soft ferromagnetic materials,” *IEEE Trans. on Magnetics*, Vol. 24, No. 1, 621–630, 1998.
  15. Anders, G.-J., *Rating of Electric Power Cables: Ampacity Computations for Transmission, Distribution and Industrial Applications*, New York, 1997.
  16. IEC Standard 60287, *Electric Cables — Calculation of the Current Rating — Part 3-2: Sections on Operating Conditions — Economic Optimization of Power Cable Size*, 2nd edition, 2006.